

Possibility of a photometric detection of “exomoons”

Gy. M. Szabó,^{1,2} K. Szatmáry,¹ Zs. Divéki¹ and A. Simon¹

¹ Department of Experimental Physics & Astronomical Observatory, University of Szeged, 6720 Szeged, Hungary
e-mail: szgy@titan.physx.u-szeged.hu

² visitor at the Harvard-Smithsonian CfA, Cambridge, MA

ABSTRACT

Aims. We examined which exo-systems contain moons that may be detected in transit.

Methods. We numerically modeled transit light curves of Earth-like and giant planets that contain moons with 0.005–0.4 Earth-mass. The orbital parameters were randomly selected, but the entire system fulfilled Hill-stability.

Results. We conclude that the timing effect is caused by two scenarios: the motion of the planet and the moon around the barycenter. Which one dominates depends on the parameters of the system. Already planned missions (Kepler, COROT) may be able to detect the moon in transiting extrasolar Earth-Moon-like systems with a 20% probability. From our sample of 500 free-designed systems, 8 could be detected with the photometric accuracy of 0.1 mmag and a 1 minute sampling, and one contains a stony planet. With ten times better accuracy, 51 detections are expected. All such systems orbit far from the central star, with the orbital periods at least 200 and 10 days for the planet and the moon, while they contain K- and M-dwarf stars. Finally we estimate that a few number of real detections can be expected by the end of the COROT and the Kepler missions.

Key words. Planets and satellites: general - Methods: data analysis - Techniques: photometric

1. Introduction

The photometric transit detection of exoplanets has become an effective tool in the past 6 years. The known systems (9 transits up to now) are summarized in the Schneider catalogue (2005). In the future a few programs are planned to achieve measurements that are as accurate as ca. 0.01–0.1 mmag, allowing the detection of a large sample of Earth-like planets while they are in service (e.g. COROT mission, Auvergne et al., 2003, Kepler mission, Borucki et al., 2003, Basri et al., 2005). The power of photometric detection is expected to keep increasing in the future.

Sartoretti & Schneider (1999, SS99), Deeg (2002, D02), and Doyle & Deeg (2003) argue that a larger moon than the Earth that is orbiting around an exoplanet causes measurable photometric effects. Although there are only negative ground-based observations (Brown et al., 2001, Charbonneau et al., 2005), it is expected that the planned space missions will be able to discover the exomoons.

2. Light curve simulations

Light curve calculation consisted of modeling dynamically stable planet-moon (P–M) systems around real star models. The star models were based on the latest Padova isochrones (Girardi et al., 2002), supplemented with Phoenix linear limb darkening coefficients (Claret, 2000). Both the planet and the moon had circular orbits, with the inclination taken into account. The other input model parameters were (i) the age and suspected metallicity of the star, (ii) the orbital periods, masses, and radii of the planet and the moon, and (iii) the photometric filter of the modeled observation.

So as to exclude the short-time escape of the moon, the system had to fulfill Hill stability. According to it, the a_{moon} radius of the moon was inside the L2 Lagrangian-point; and the C_2 Jacobi-constant at L2 was smaller than for the orbiting moon, so the total energy balance prohibited escaping through L2. Mathematically

$$C_{\text{moon}} \equiv 2\Omega_{\text{moon}} - v_{\text{moon}}^2 > C_{L2}, \quad (1)$$

where the effective potential $\Omega(x, y)$ denotes the same as is common for the circular restricted TBP, v is the velocity of the moon, and C_{L2} is simply $2\Omega_{L2}$.

The first step in modeling was to determine the radius of the star from the input parameters. Then the radii of

orbits were calculated for the star–planet and the planet–moon systems according to Kepler’s third law. Although the exact solution of the moon’s orbit requires solving a three-body problem (TBP), we included an approximation when the planet and the moon were orbiting with uniform velocity around their barycenter. This approximation is good to the third order in the distance ratio (i.e. moon–planet to planet–star) and in time, and is fully acceptable within the needs of the main problem.

The apparent stellar flux during the transit was evaluated from a simulated image of a real star model star in which pixels are zeroed by the transiting objects. The stellar diameter was 1000 pixels, and fluxes were normalized to out-of-transit stellar flux.

A sample light curve pair is presented in Fig. 1. The mass of the central star is $0.7 M_{\odot}$, while the planet and the moon have similar sizes as the Earth and the Moon, respectively, the orbital velocity of the planet is 30 km/s, and the orbital period of the moon is 29 days.

When simulating observations, we sampled the previously modeled light curves discretely, and co-added adjustable Gaussian noise. This involved two more model parameters such as the sampling rate and photometric accuracy. We set them arbitrarily, and also included the expected data quality of the planned missions. This latter meant measurements with 0.1 mmag accuracy, sampled every minute. Although the standard sampling rate of Kepler will be 15 minutes, the transits will be read out once every minute for better resolution (D. Latham, private communication). The standard sampling of the COROT will be 8 minutes with the possibility of 32-second readout for each of 32 highlighted targets. We present two model observations in Fig. 2.

We calculated the timing effects according to the method of D02. Surprisingly, the method gave that the timing effect often appeared reversed (“earlier” transit with leading moon) and with larger time shifts as predicted by the previous works cited above. The reason for this turned out to be a second scenario present in the timing effect, which we describe in the following.

2.1. Timing effects

We define the τ central time of transit points as D02,

$$\tau := \frac{\sum_{transit} (t_i \cdot \Delta m_i)}{\sum_{transit} \Delta m_i} \quad (2)$$

where t_i and Δm_i are the observational times and measured differential magnitude. The summation index *transit* means that only the points belonging to the transit have to be taken into account. When the photometric points are equally sampled, τ will be the time when the planet passes before the central meridian of the star within the statistical errors. (In case of non-uniform sampling, one has to use statistical weights, but in the case of the modeled automatic measurements the sampling is uniform.) Let $\Delta T = \tau_o - \tau_c$ mean the time difference between

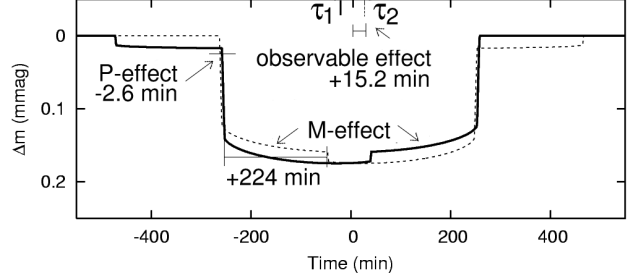


Fig. 1. A sample light curve of two transits with a leading (solid line) and a trailing moon (dashed line) with the time differences. The P-effect of -2.6 minutes is majorated by the M-effect between the transits of the moon (224 min), while the observable effect is 15.2 min.

the observed and the expected central time (calculated if the planet had no moon) of the transit.

In the presence of a moon the planet revolves around the barycenter, and some transits of the planet occur somewhat earlier or later than expected (SS99, D02). On the other hand, the same is also true for the moon: depending on its trailing or leading position, its individual transit occurs earlier or later. So as to distinguish those scenarios, we will call the timings due to transit of the planet and the moon as P-effect and M-effect, respectively.

As the moon orbits farther from the barycenter, the M-effect can exceed the P-effect in time by quite a lot, but as the moon is tiny, this effect is much less in magnitude. In practice we observe some combinations of P- and M-effects. If the moon is leading, the first half of the combined transit curve will be slightly deeper, and shallower after the moon finishes the transit (Fig. 1). The points referring to earlier times will get slightly more weight (Eq. 2.), and finally τ may refer to an earlier time. This is exactly what we found in our model observations. Even when the moon was too tiny to cause evident light curve distortions, τ could predict the presence of the moon, due to the robust averaging in Eq. 2.

The effect that has more influence on the detected transit time depends on the system parameters. If the moon is large and orbits far from the planet, the M-effect can far exceed the P-effect. For example, the P-effect is -2.6 minutes for the Sun–Earth–Moon system, its amplitude is 0.1 mmag (D02), the M-effect is 224 minutes, and its amplitude is 0.0085 mmag. The observed effect will roughly be the magnitude-weighted average, $(0.0085 * 224 - 0.1 * 2.6) / (0.1085) \approx 15.2$ minutes.

We note that the moon detection is more difficult if there is a large spot on the stellar surface. The spot can cause light curve variations thus τ may vary without the presence of a moon.

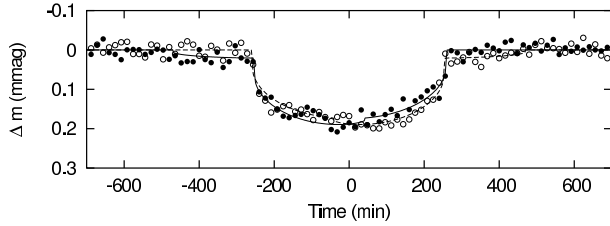


Fig. 2. Simulated observations (0.1 mmag-quality, 1 min sampling, 15 min averages for perspicuity) showing the central transit of an Earth-sized planet and a Moon-sized moon before a $0.7M_{\odot}$ star (dots: leading moon, circles: trailing moon).

3. Detectable systems

3.1. The Earth–Moon-like systems

Will the mission Kepler be able to find Earth–Moon-like systems around solar-like stars? The photometric effect of the Moon is 0.0085 mmag, so compared to the photometric accuracy of about 0.01–0.1 mmag the answer would be “no”. But there is hope for the detection of a Moon-sized moon around an Earth-sized exoplanet, due to the combined effect exceeding 15 minutes. We simulated 0.1 mmag-quality measurements with 1-minute samplings. The observed scenario was similar to Fig. 2, but with smaller amplitudes because the central star was $1 M_{\odot}$. We calculated 20 events consisting of 4–4 neighboring transits, and randomized the initial orbital phase of the moon. We found 5 detections in 20 calculations – this detection is not very probable, but cannot be excluded.

We defined a similar system in order to decide whether the photometric accuracy or the sampling rate is more dominant (Fig. 2) for a successful detection. We selected a $0.7 M_{\odot}$ central star with $t = 5$ Gyr and $Z = 0.019$ metal content, while the planet and moon masses, sizes, and periods were the same as for the Earth–Moon. It was found that the success of the detection was primarily determined by the sampling rate. Even with the 0.1-mmag photometric accuracy, we got a 3σ detection if the sampling rate was 1 or 2 minutes. In contrast, no positive detection was found with a 30-minute sampling rate, and the positive detections with 10 and 20-minute sampling rates were also rather ambiguous (Fig. 3).

3.2. Other detectable systems

From an observational point of view, it is interesting to characterize systems that contain observable moons. We applied a Monte-Carlo method for finding some appropriate systems. We randomly generated systems, simulated the transits, and checked if the moon is observable with at least 3σ confidence. Five hundred systems were modeled containing both giant and Earth-like planets, different inclinations, planet and moon densities, and orbital periods, where the period of the planet did not exceed 400 days in order to have at least 4 transits during the planned opera-

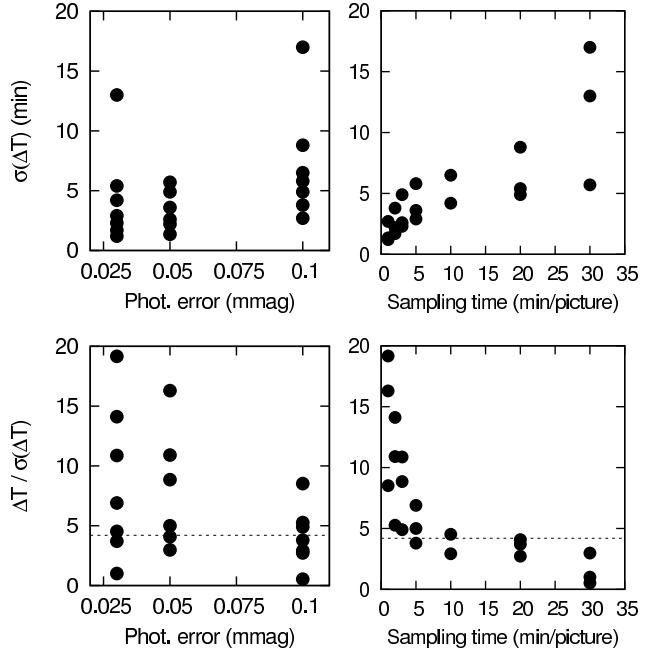


Fig. 3. Uncertainties of the timing effect in the described Earth–Moon-like system. Top: the panels show the 1σ ambiguities of the time delays as a function of photometric accuracy (left panel) and of sampling interval (right panel). Bottom: the same but expressed in relative errors; the simulations leading to 3σ positive detections are above the dashed line.

tion time of Kepler. One set of model measurements were calculated with the “present” (0.1 mmag) accuracy with a 1-minute sampling rate, and a “future observable” set was included with ten times better accuracy (0.01 mmag).

We found 51 “future observable” systems and 8 that could be observed with the “present” accuracy. Both giant and Earth-like planets can have observable moons; in the first case the S/N of the transit is high enough to allow accurate measurement. In the second case the combined effect exceeds a few (5–55) minutes as the masses of the moons were comparable to the mass of the Earth-like planet. The present equipments allow the detection of 5 moons of giant planets around red dwarf stars, but a positive detection suggests that there is a chance in the case of Earth-like planets. The planet has to be at least 0.6 AU from the star when observing with the present accuracy, and at least 0.4 AU in the case of the ten-times accurate measurements.

The present equipments allow detection of the moons of giant planets around red dwarf stars (Fig. 4., left panel), but positive detections suggest that there is some chance in case of Earth-like planets, or even detections for G-stars. The “future observable” systems contain more detections with an Earth-like planet, while they seem to allow more positive detections for G- and K-stars, too. There is also an upper limit to the photometric accuracy: when the modelled light curves had 0.15 mmag accuracy

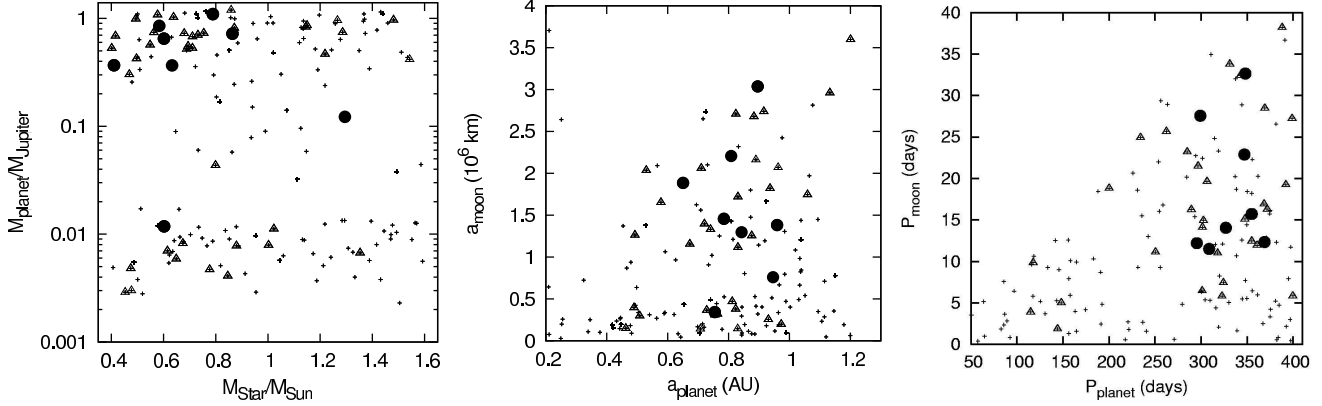


Fig. 4. Systems with a detectable moon, if the photometric accuracy is 0.1 mmag (large dots) or 0.01 mmag (triangles); undetectable systems are marked by small crosses.

and so a bit less S/N, only 3 moons were positively detected.

The middle panel confirms another important restriction: the semi-major axis of the planet has to be large enough (0.6 AU with 0.1 mmag-quality, 0.4 AU with 0.01 mmag). The planets farther from the central star move more slowly, and they can have more distant Hill-stable moons. Both make detection easier. Experimentally, almost every third test system was positively detected where the moon was farther than one million km from the planet (referring to the 0.01-mmag simulated accuracy).

The right panel expresses the same in terms of orbital periods: the planet must have at least about 280 days orbital period for promising detections. This is not too favorable as one can expect only a few transits during a 4-year mission, thereby reducing the chance for a somewhat detailed modeling of the moon itself.

This condition makes the detection of a moon around the well-known “hot-Jupiter” planets quite unlikely. Those planets revolve so fast that the combined effect lies within the magnitude of a second. The only way to make a detection would be with the shape variation: for the smallest ($0.7 R_{\odot}$) central star, OGLE-TR113, the photometric effect of a Ganymede-sized moon is less than 0.03 mmag, and only 0.2 mmag for an Earth-sized moon. Their Hill-radius is rather small, extending only to twice the radius of the planet, so the probability of a moon being present is low. Considering their extended atmosphere as well, which may decelerate an orbiting body, the “lifetime” of any moon seems to be limited.

4. Conclusions

What is the suggested observational strategy in order to find exomoons? Although the required photometric accuracy (0.1–0.15 mmag) seems to be about the highest quality we can expect nowadays, short sampling intervals should be used whenever possible. This will help by increasing the number of systems where the timing effect is less, e.g. when the moon is smaller, closer to the planet,

or the mass ratio is smaller. The strategy of the planned missions is concordant with this.

We note that the observing strategy of Kepler (Basri et al., 2005) may allow the detection of exomoons, but may also lead to the rejection of those observations. The transit pipeline of Kepler includes at least 3 transits with timings that are consistent with a periodically revolving planet, within the observational errors. Any inconsistent transits will be rejected. If an exomoon has an observable timing effect such that timings occur *discordantly* under the assumption of strict monoperiodicity, Kepler may not recognize the light variation as a transit. Therefore we suggest including some timing variation in the acceptance criteria.

The possible spectroscopic confirmation of a moon could be either the observation of the perturbations in the radial velocity of the star or the detection of the moon within the Rossiter-McLaughlin effect, which e.g. Bouchy et al. (2005) observed for a transiting planet. Unfortunately both mean only slight variations in the fine structures, which is why there is really little hope for their success.

Based on the presented calculations, one may estimate the magnitude of the expected real detections with Kepler. The total number of Earth-sized planets to be discovered is a few hundred during the entire mission. If only 5 percent of them have a moon similar to our Moon, and only every fifth moon are really found, we should get a few positively detected exomoons. If we take the COROT mission and the forthcoming missions into account, we may have a few dozen known exomoons by the end of the following decade.

5. Acknowledgements

The research was supported by Hungarian OTKA Grant T042509. We thank D. W. Latham for his hospitality and for the fruitful discussions.

References

- Auvergne, M., Boisnard, L., Buey, J-T. M., et al., 2003, SPIE, 458, 170
- Basri, G., Borucki, W.J., Koch, D., 2005, NewAR, 49, 478
- Bouchy, F., Udry, S., Mayor, M., et al., 2005, astro-ph/0510119
- Brown, T.M., Charbonneau, D., Gilliland, R.L. et al., 2001, AJ, 552, 699
- Borucki, W.J., Koch, O.G., Lissauer, J.J., 2003, SPIE, 458, 129
- Charbonneau, D., Winn, J.N., Latham, D. W. et al., 2005, astro-ph/0508051
- Claret, A. 2000, A&A, 363, 1081
- Deeg, H.J., 2002, ESA publ. SP-514, 237 (D02)
- Doyle, L.R., Deeg, H.J., 2003, IAUS, 213, 80
- Girardi, L., Bertelli, A., Bressan, C. et al., 2002, A&A, 391, 195
- Sartoretti, P., Schneider, J., 1999, A&AS, 134, 550 (SS99)
- Schneider, J., 11 October 2005,
<http://vo.obspm.fr/exoplanetes/encyclo/catalog.php>